A Novel Method for Output Characteristics Calculation of Electromagnetic Devices using Multi-kernel RBF Neural Network

Feng Ding, Yunyun Gao, and Jianhui Tian

Department of Mechanical and Electronic Engineering
Xi'an Technological University, Xi'an, 710021, China
dd_feng@sina.com, 1032660865@qq.com, carl8@qq.com

Abstract ─ The action performance and reliability of electromagnetic devices is critical to the entire working system. In this paper, a new method for calculating the output characteristics of electromagnetic devices is proposed. This method uses the multi-kernel radial basis function neural network (MK-RBFNN) approximation modeling by the finite element calculation results at the key nodes. It obtains the output response of the electromagnetic device under different coil voltages and air gaps. The key of establishing a MK-RBFNN is to obtain the weight coefficients of each single-kernel radial basis function (RBF) model by using a heuristic weighting strategy. When the electromagnetic output characteristics is calculated in the optimization design of the electromagnetic device, this method solves the problem that the traditional method is difficult to balance the calculation accuracy and speed. The effectiveness of the method is verified by the calculation results of the electromagnetic torque of a typical electromagnetic relay.

Index Terms ─ Electromagnetic device, finite element, multi-kernel radial basis function, neural network, optimal design.

I. INTRODUCTION

The key to the optimal design or robust design of the electromagnetic device is to analyze the influence of the input parameters on the output characteristics, and it is necessary to repeatedly calculate the static characteristics [1]. The existing methods for solving output characteristics of electromagnetic devices mainly include magnetic equivalent circuit method (MEC), finite element method (FEM) and approximation model, but they all need to be further improved. In this paper, the multi-kernel RBF neural network is used to solve the output characteristics of the electromagnetic device, which can further improve the calculation speed while ensuring the calculation accuracy.

The traditional MEC has high computational efficiency but its calculation accuracy is not good because of neglecting magnetic flux leakage and magnetic saturation. Therefore, many researchers have conducted research in recent years to improve the calculation accuracy of MEC. Amrhein and Krein [2] used the magnetic resistance network method to establish a three-dimensional magnetic circuit model of the electromagnetic device based on the distribution of the spatial magnetic field. However, this method complicates the analysis of the magnetic circuit and increases the amount of calculation for non-linear solutions. It still has not improved the calculation efficiency.

The high accuracy and time-consuming characteristics of FEM make it difficult to adapt to a robust design or optimization process. The researchers tried to combine the advantages of FEM and MEC to establish an approximate model of the electromagnetic output response. Encica et al. [3] used the idea of spatial mapping to construct a geometric model whose matching result matched the finite element. However, it is difficult to establish a mapping relationship in a complex magnetic circuit with multiple design parameters.

The wide application of intelligent algorithms has led researchers to try to establish an approximate model through mathematical methods to achieve rapid calculation of electromagnetic characteristics. Xia et al. [4] constructed the Kriging approximation model of the electromagnetic device and optimized the parameters of the superconducting coil. The accuracy of the Kriging method depends on the choice of the basis function type. However, there is currently no uniform method to select this basis function. An approximate model of the electromagnetic device obtained using the custom interpolation function is presented in [5]. This method uses a custom interpolation function, but it is difficult to construct a suitable interpolation function according to different electromagnetic devices.

In 1989, Jackson demonstrated the approximation performance of Radial basis function (RBF) neural networks for nonlinear continuous functions. Papers [6,7] showed the advantages of RBF neural networks in predicting compared to other neural networks through experiments in different fields. Benbouza [8] explored the effects of radial basis functions in the field of

electromagnetic computing. Papers [9] improved the existing RBF neural network to meet the needs of different occasions. A number of studies have shown that the RBF approximation model has higher predicting accuracy than other approximation models in the case of linearity, weak nonlinearity and strong nonlinearity. These findings provide support for the application of RBF neural networks in the field of electromagnetic device computing.

This paper aims to propose a new method for calculating the output characteristics of electromagnetic devices quickly and accurately. The method adopts the idea of approximate modeling. By selecting the finite element calculation results at key nodes as sample points, a MK-RBFNN is constructed to determine the output characteristics (electromagnetic torque) of electromagnetic devices under different coil voltages and air gaps. As a case study of the clapper-type electromagnetic mechanism of a typical electromagnetic relay, the accuracy and rapidity of the method are verified significantly and effectively.

II. METHOD DESCRIPTION

The implementation steps of the novel method proposed in this paper are shown in Fig. 1. It makes great use of the advantages of each single-kernel RBF neural network, which can quickly and accurately calculate the output characteristics of the electromagnetic device.
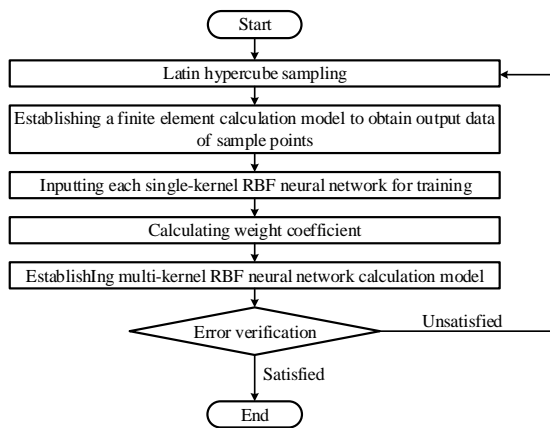

Fig. 1. Flow chart of method for output characteristics calculation of electromagnetic device.

A. Latin hypercube sampling
(a) Determining input variables and output variables
The appropriate input variables and output variables must be selected before the test design, which is the premise of the approximate numerical calculation. Taking a rotating electromagnetic device as an example, the differential equation of electromagnetic output characteristics can be established by the voltage balance equation and the D'Alembert [10] equation of motion,

the expression is:

$$\begin{cases} u_0 = i(\psi,\theta)R + \dfrac{d\psi}{dt} \\ J\dfrac{d\omega}{dt} = T(U,\theta) - T_f(\theta) \cdot \\ \omega = \dfrac{d\theta}{dt} \end{cases} \quad (1)$$

In (1), u_0 is the power supply voltage of the coil circuit; i is the current of the coil; R is the resistance of the coil; ψ is the flux linkage; J is the torque of inertia; ω is the angular velocity; U is the voltage of the coil; θ is the rotation angle of armature; T is the electromagnetic torque; T_f is mechanical torque.

The coil voltage U and the rotation angle θ of armature of the electromagnetic device will vary over time during operation. In the dynamic characteristic calculation process, it is necessary to analyze the electromagnetic characteristics corresponding to different voltages U and different rotation angles θ. U and θ in (1) have two conditions: static (U and θ are fixed), dynamic (U and θ follow Change of time).

Therefore, the voltage U and the rotation angle θ are input variables, and the electromagnetic torque T of the armature is the output variable when calculating the output characteristics of the rotating electromagnetic device.

(b) Generating sample data
The basis of constructing the approximate model is sample data. The appropriate number of experimental data with uniform distribution can better reflect the information of the whole space. Conversely, improper sample data will result in a model with poor fitting accuracy, and even get the wrong model, so it is especially important to choose the appropriate experimental design method.

The Latin hypercube sampling (LHS) [11] method was proposed by M. D. McKay and R. J. Beckman in 1979. The LHS is a method of approximately random sampling from a multivariate parameter distribution. The basic principle is: if N sample points need to be collected, then the interval with m variables is divided into N intervals with equal probability, take a random value for each variable in each interval, so each variable has N values. Finally, the N values of m groups are randomly combined into a whole sample.

The LHS steps can be summarized as the following three steps:

i) Selecting the parameters to be sampled. Such as the rotation angle θ of armature and the voltage U of coil.

ii) Generating random number. Each variable x_i is divided into K non-overlapping intervals with equal

probability, the probability of each interval is $1/k$, then a representative parameter x_i^k is generated from each subinterval with equal probability. This parameter is usually the midpoint of the interval.

iii) Generating samples. The representative samples of each parameter x_i^k are arranged by random number. Thus, N random combinations are formed, each of which contains a representative sample x_i^k of all variables.

The LHS ensures that the sample points taken represent the entire design space, and each level of each design variable is considered only once. Therefore, the sample points obtained by this method are less repetitive, and the number of samples can be set flexibly, which has good sampling efficiency and balance performance. This paper uses the LHS method for initial sampling based on the above advantages when establishing an approximate calculation model for electromagnetic devices.

B. Establishing finite element calculation model

The solution of electromagnetic field is generally based on Maxwell's equations, and the FEM is one of the most advanced and powerful methods for solving Maxwell's equations [12]. FLUX is the leading simulation software for electromagnetic and thermal calculations based on finite element theory developed by Altair [13].

The simulation calculation process includes geometry, meshing and physical description, these preparations make the established model as close as possible to the real model. The basic steps of establishing the finite element model of electromagnetic equipment with the FLUX are shown in Fig. 2.
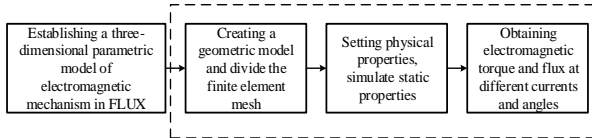

Fig. 2. Basic steps of constructing a finite element calculation model.

According to the finite element model established by FLUX software, the output response value of each input variable sample is calculated to form the sample set of corresponding output variables.

C. Inputting each single-kernel RBF neural network for training

In recent years, RBF have been widely studied in the field of neural networks. Their excellent interpolation quality has led to their application in computational electromagnetics [14]. The expression of the RBF is:

$$\hat{y}(x) = \beta_0 + \sum_{i=1}^{N} \beta_i \varphi\left(\| x - x_i \|\right). \quad (2)$$

In (2), β_0 is a polynomial function (determined form), N is the size of the hidden layer, and its value generally does not exceed the number of sample points, β_i is the weight value between the i-th input layer neuron and the p-th hidden layer neuron, φ is the kernel function, also known as the transfer function of the hidden layer, x_i is the center of hidden layer node of neural network, $\|\|$ is Euclidean distance.

It is worth noting that the determination method of center x_i. After testing, the commonly used k-means clustering algorithm is not ideal, and its global accuracy is poor. In this paper, the center x_i is determined based on the orthogonal least square (OLS) method. Because OLS finds the best function of matching data by minimizing the sum of squares of errors, it is possible to control the fitting accuracy by setting errors during the training process, and adaptively determine the number of hidden nodes according to the error requirements. On the contrary, in the process of using the k-means clustering algorithm, the number of hidden nodes needs to be determined first. Different values have a great influence on the results of the fitting calculation, which is inconvenient for the application of the method in this paper.

The kernel functions commonly used in the RBF model are shown in Table 1 [15]. r represents the Euclidean distance between x and center x_i. The shape parameter c can be specified by experience.

Table 1: Commonly used kernel functions in the RBF model

Name	Expression	Abbreviation
Linear Function	$\varphi(r) = r$	LN
Cubic Function	$\varphi(r) = (r + c)^3$	CB
Thin Plate Spline	$\varphi(r) = (r^2 + c^2) \ln(r + c)$	TPS
Multi-quadric Function	$\varphi(r) = \sqrt{r^2 + c^2}$	MQ
Inverse Multi-quadric Function	$\varphi(r) = \dfrac{1}{\sqrt{r^2 + c^2}}$	IMQ
Gaussian Function	$\varphi(r) = e^{-\frac{r^2}{2c^2}}$	GA

According to the test, the application effect of the last four kernel functions in Table 1 is better. The single-kernel RBF neural network with them as kernel functions has a good fitting effect on the output characteristics of electromagnetic equipment.

D. Establishing MK-RBFNN calculation model
(a) Introduction of MK-RBFNN model

The RBF model has strong nonlinear mapping ability and optimal function approximation performance, and has fast calculation speed. However, further research shows

that its robustness is poor, so it is necessary to choose different kernel functions to build RBF model according to different problem types. In view of the above shortcomings, this paper proposes a MK-RBF model constructed by multiple kernel functions based on the merits of each kernel function. This model has higher fitting precision and stronger robustness than the general RBF model constructed by a single kernel function.

According to the four kernel functions mentioned in Section IIC, the MK-RBFNN model is established. The expression are:

$$\begin{cases} \hat{y}_{MK-RBF}(x) = \sum_{i=1}^{M} \lambda_i \hat{y}_i(x) \\ \sum_{i=1}^{M} \lambda_i = 1 \end{cases}. \qquad (3)$$

In (3), M is the number of single-kernel RBF models needed to construct the final MK-RBF neural network model, $\hat{y}_{MK-RBF}$ is the predicted value of the MK-RBF neural network model, $\hat{y}_i(x)$ is the predicted value of the i single-kernel RBF neural network model, and λ_i is the weight coefficient corresponding to the i single-kernel RBF neural network model.

The establishing structure of the multi-kernel RBF neural network model are shown in Fig. 3.
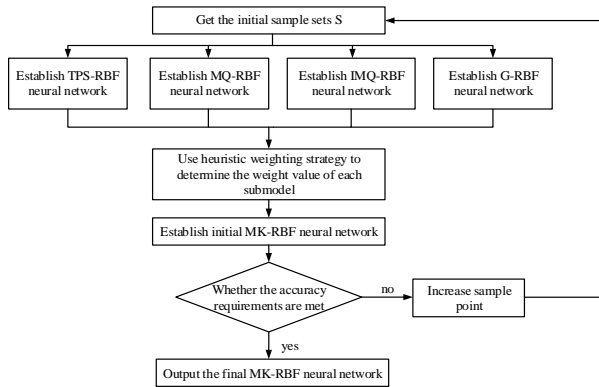

Fig. 3. Establishing structure of MK-RBFNN model.

(b) Calculating weight coefficient
The weight coefficient is very important in constructing the final approximation model. The heuristic weighting strategy can better balance the weight values of each single-kernel RBF model, and can make the final MK-RBF model get better fitting effect. The basic expressions are:

$$\begin{cases} \lambda_i = \lambda_i^* \Big/ \sum_{i=1}^{M} \lambda_i^* \\ \lambda_i^* = \left(E_i + \alpha E_{avg} \right)^{\beta} \\ E_{avg} = \frac{1}{M} \sum_{i=1}^{M} E_i \end{cases}. \qquad (4)$$

In (4), $\alpha < 1, \beta < 0$, α and β respectively represent parameters that have a large influence on the degree of emphasis on the constituent model. A smaller α values and a larger $|\beta|$ values indicate higher weights for single-kernel RBF models with higher prediction accuracy. A larger α value and a smaller $|\beta|$ value indicate a higher average confidence for each single-kernel RBF model. According to experience, this paper takes $\alpha = 0.05, \beta = -1$, so that each single-kernel RBF model has the optimal weight coefficient. In this paper, E_i is generally obtained by Generalized Mean Square Cross-validation Error (*GMSE*). The expression is:

$$E_i = \sqrt{GMSE_i} = \sqrt{\frac{1}{k} \sum_{j=1}^{k} \left(f_j - \hat{f}_j^{(-j)} \right)^2}. \qquad (5)$$

In (5), k represents the total number of sample points taken by the i-th single-kernel RBF model, and $\hat{f}_j^{(-j)}$ represents the predicted value of the i-th single-kernel RBF model at point $x^{(j)}$, which is constructed by the remaining $k-1$ points (excluding point $\left(x^{(j)}, f_j \right)$).

E. Error verification
In the case of a fixed number of sample points, the researchers usually use some error indicators to evaluate the fitting accuracy of the approximate model. The error is further divided into relative error and absolute error. When the value of a certain type of data is originally small, the relative error can well characterize the fitting accuracy. Therefore, this paper chooses the relative error with strong applicability.

In this paper, two global error indicators and one local error indicator are used to evaluate the performance of the model, as follows:
a) Coefficient of multiple correlation (R^2):

$$R^2 = 1 - \frac{\sum_{i=1}^{m}(y_i - \hat{y}_i)^2}{\sum_{i=1}^{m}(y_i - \bar{y})^2} = 1 - \frac{MSE}{Var}. \qquad (6)$$

b) Relative root mean square error (*RRMSE*):

$$RRMSE = \frac{1}{STD} \sqrt{\frac{\sum_{i=1}^{m}(y_i - \hat{y}_i)^2}{m}}. \qquad (7)$$

c) Relative maximum absolute error (*RMAE*):

$$RMAE = \frac{\max_{i=1,2,...,m} |y_i - \hat{y}_i|}{STD}. \qquad (8)$$

Where m represents the number of points sampled when validating the model, y_i represents the true value, $\hat{y}_i$ represents the predicted value obtained by the established model, and $\bar{y}$ represents the average of all true values. *MSE*, *Var*, and *STD* represent the mean square error, the variance of the true value, and the

standard deviation, the calculation expressions are:

$$MSE = \frac{\sum_{i=1}^{m}(y_i - \hat{y}_i)^2}{m} \; , \qquad (9)$$

$$Var = \frac{\sum_{i=1}^{m}(y_i - \bar{y})^2}{m} \; , \qquad (10)$$

$$STD = \sqrt{Var} \; . \qquad (11)$$

The global error indicators R^2 and *RRMSE* are all related to the *MSE*. As can be seen from the above formulas, a larger R^2 and a smaller *RRMSE* indicate a smaller *MSE*. The approximate model established at this time has a small global error and a high prediction accuracy. The local error indicator *RMAE* characterizes the local fitting accuracy of the approximate model. The smaller *RMAE* indicates that the approximate model has higher fitting accuracy. Otherwise, it indicates that the approximation model has poor fitting accuracy in a certain region.

III. APPLICATION EXAMPLE: OUTPUT CHARACTERISTIC CALCULATION OF ELECTROMAGNETIC RELAY

A. Introduction to application example

Aiming at the above mentioned calculation method of multi-core radial basis function neural network applied in the field of electromagnetic calculation, this paper takes ARM2F relay as the research object, establishes a fast calculation model of armature electromagnetic torque of its electromagnetic system, in order to verify the effectiveness of this method. As shown in Fig. 4, the electromagnetic system of ARM2F relay belongs to a typical clapper-type electromagnetic structure, which is composed of yoke iron, armature, iron core and coil.
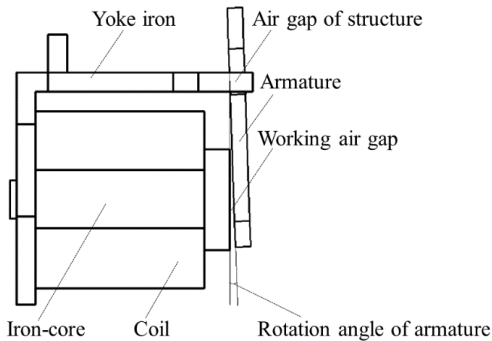
Fig. 4. Structure of the ARM2F electromagnetic system.

B. Method application

The geometry of the coil is established in flux, and the input parameters of the coil are automatically generated by the software. Then, through generating

grid, applying voltage (current), adding material B-H characteristics and other parameters, the software gets the flux density based on the finite element method, and gets the electromagnetic torque of the armature in the post-processing module.

Taking the magnetic flux density of the electromagnetic mechanism with the 6V voltage and the rotation angle of armature at 2.1° as an example, the calculated flux density is shown in Fig. 5.

In the range $(0 \le U \le 24\text{V}, 0 \le \theta \le 2.1°)$ of input parameters of electromagnetic system, 44 groups of sample points of input parameters are obtained by Latin hypercube sampling, and the output response of input samples is calculated by FLUX software to form the initial sample set S.
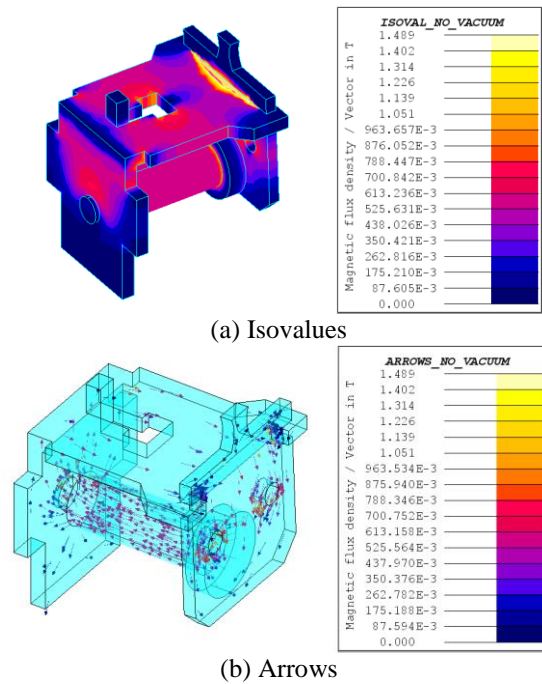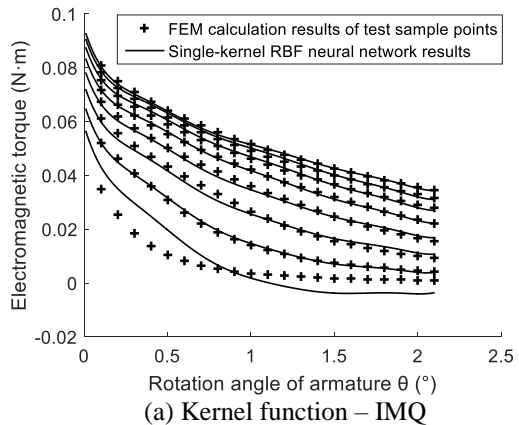
(a) Isovalues

(b) Arrows

Fig. 5. Magnetic flux density (Isovalues and Arrows).

(a) Kernel function – IMQ

(b) Kernel function – MQ

(c) Kernel function – TPS
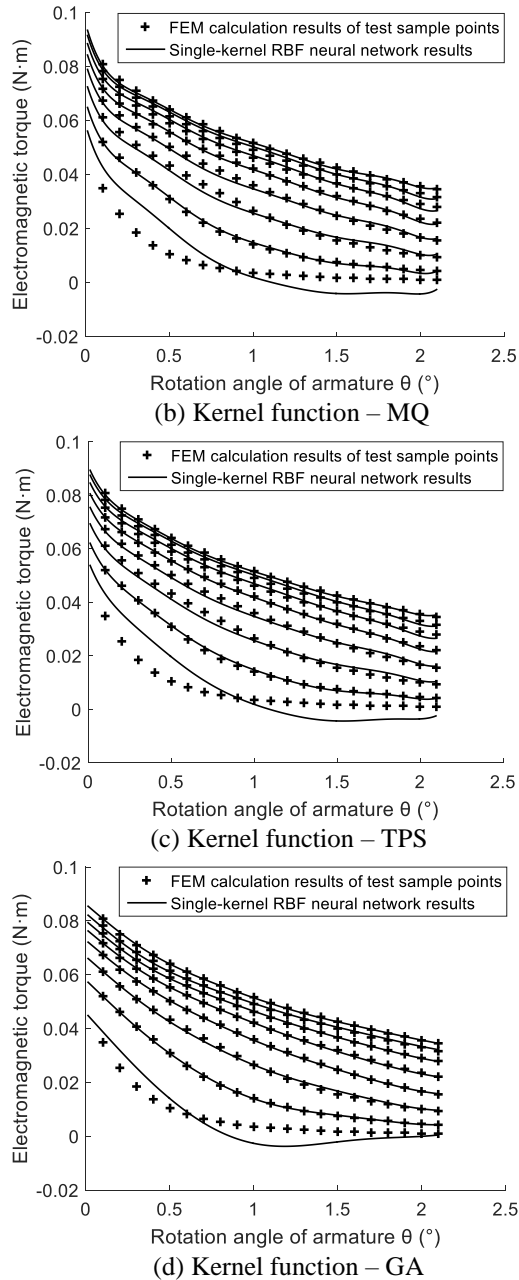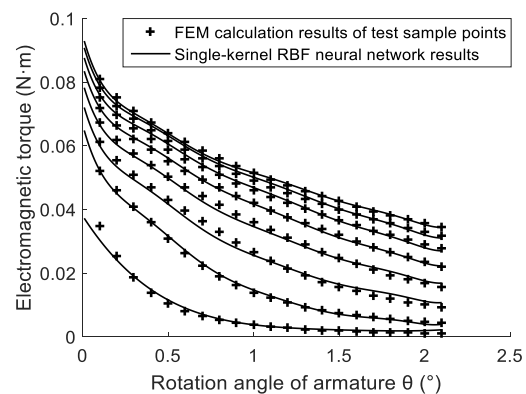

(d) Kernel function – GA

Fig. 6. Comparison of four single-kernel RBF neural network results and the FEM calculation results of test sample points.

The sample set S is input into the single-kernel RBF neural networks with four different kernel functions for training, and four kinds of single-kernel RBF neural networks are obtained. 168 test sample points are taken at equal intervals within the range of input parameters of
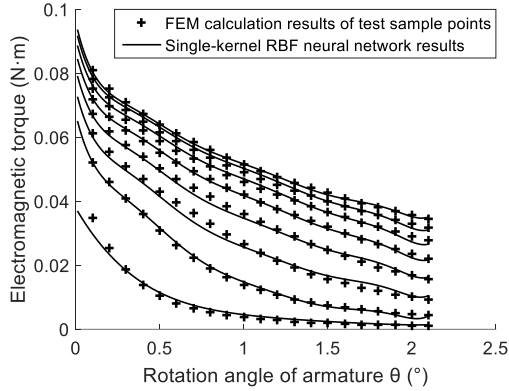
electromagnetic system, and the output response of test sample points is calculated by using the software of FLUX. The comparison between the calculation results of different single-kernel RBF neural network and the test sample results calculated based on the FEM is shown in Fig. 6. The total 8 curves in Fig. 6 represent the relationship between the rotation angle of armature and the output electromagnetic torque when the voltage is 24V, 21V, 18V, 15V, 12V, 9V, 6V and 3V respectively. The RBF neural network models established with different kernel functions are shown in (a), (b), (c), and (d) of Fig. 6. The kernel functions are IMQ, MQ, TPS, and GA.

It can be seen from Fig. 6 that the calculated results of the RBF neural network trained by four different kernel functions are roughly the same as those of the finite element calculation of the test point in the range of 6V-24V. But in the case of voltage below 6V, there is a large deviation. Low voltage will lead to a sharp decrease in the main flux of the coil, and the nonlinearity of electromagnetic torque with the change of rotation angle of armature is much higher than that of high voltage. Therefore, a small number of sample points make the prediction accuracy of RBF neural network sharply reduced in this range.
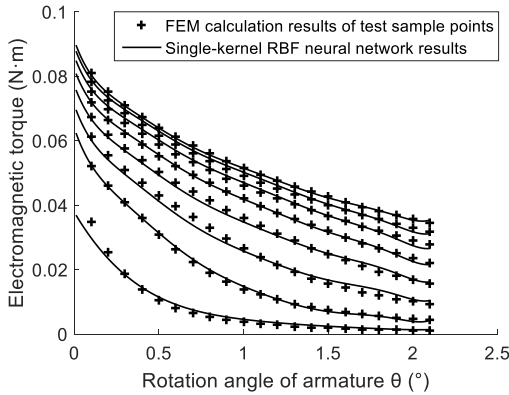
In order to solve the problem of excessive local deviation, this paper constructs different neural networks in different intervals. For the part below 6V, increasing the sample points for neural network training. Specifically, in the voltage range of 0V-6V, 11 sampling points are obtained through LHS again. In this interval, an RBF neural network is additionally constructed with a similar kernel function to reflect the response of the electromagnetic torque to the armature rotation angle in this range. Ultimately, two RBF neural networks are constructed by using 55 samples in two intervals to calculate the output response in the whole range of input parameters. The final calculation results of this scheme are shown in Fig. 7.
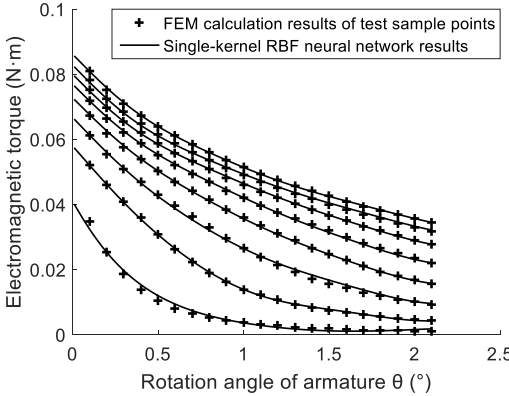

(a) Kernel function – IMQ (two parts of RBFNN)

(b) Kernel function – MQ (two parts of RBFNN)

(c) Kernel function – TPS (two parts of RBFNN)

(d) Kernel function – GA (two parts of RBFNN)

Fig. 7. Comparison of two parts of four single-kernel RBF neural network results and the FEM calculation results of test sample points.

It can be seen from Fig. 8 that the accuracy of the results calculated by the two-part neural network constructed by using the separated interval is significantly improved within the voltage of 6V. In order to balance the calculation accuracy in the global range of parameters, the MK-RBF neural network model constructed by multiple kernel functions is established by the method described in Section II. The weight coefficients of each

single-kernel RBF neural network are calculated as shown in Table 2. The final calculation results of MK-RBF neural network and the FEM calculation results of test sample points are shown in Fig. 8.

Table 2: The weight coefficient of each single-kernel RBF neural network

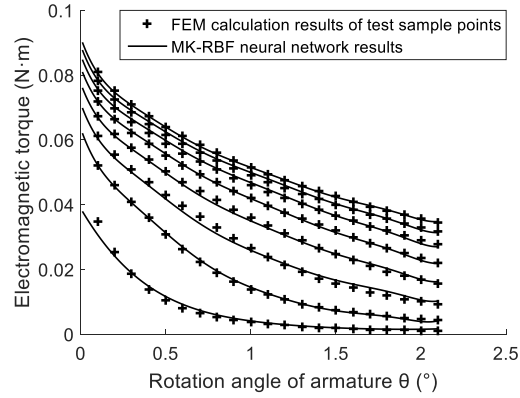| Type of Single-kernel RBF Neural Network	Weight Coefficient λ
IMQ-RBF	0.21608
MQ-RBF	0.24299
TPS-RBF	0.24292
GA-RBF	0.29801

Fig. 8. Comparison of MK-RBF neural network results and the FEM calculation results of test sample points.

C. Analysis of calculation results of application example

The calculation accuracy of MK-RBF neural network can be reflected by the error evaluation indicator. If the model has a large R^2 and a smaller $RRMSE$ and $RMAE$, which means that the model has higher prediction accuracy and fitting accuracy. 224 error test sample points are randomly selected in the range of input parameters, and the output response (electromagnetic torque) of test sample points is calculated by finite element method. Finally, the error results of RBF neural network with different kernel functions are shown in Table 3.

Whether it is to observe the comparison with the finite element results, or to compare the error evaluation indicators, it is found that the accuracy of each single-kernel RBF neural network within the different variation range of the input variables is different. For example, the IMQ-RBF and MQ-RBF neural networks have higher calculation accuracy than the TPS-RBF and GA-RBF neural networks under the conditions of an armature rotation angle of 0.1° or below it. In the working condition about the rotation angle of armature of 0.1° or over it, it is obvious that the GA-RBF neural network has

higher calculation accuracy than the other three single-kernel neural networks.

Table 3: Error results of RBF neural network with different kernel functions

Evaluation Indicator	IMQ-RBF	MQ-RBF	TPS-RBF	GA-RBF	MK-RBF
R^2	0.99629	0.99567	0.99574	0.99529	0.99704
RRMSE	0.06086	0.06582	0.06525	0.06857	0.05442
RMAE	0.34876	0.36196	0.36784	0.29412	0.32147

After the coil of the electromagnetic relay is excited by the rated voltage, with the increase of time, the rotation angle of the armature gradually approaches to 0°, the voltage gradually rises to its rated voltage, and the electromagnetic torque of the armature gradually tends to the maximum value. So it is very important to accurately calculate the electromagnetic torque at high voltage and small angle. In this case, the calculation accuracy of MK-RBF neural network model is better than GA-RBF when the rotation angle of armature is within 0.1°. In 0.1°-2.1°, the calculation accuracy of MK-RBF neural network model is better than that of the other three RBF neural networks because of the addition of GA kernel function, which has reached a satisfactory level as a whole.

It can be seen from Table 3 that the global error performance of the MK-RBF neural network is much better than any single-kernel neural network, and the local error can be controlled within a certain range. It combines the advantages of each single-kernel neural network and enhances the robustness of the calculation.

IV. CONCLUSIONS

Aiming at the need of rapidity and accuracy of the calculation process, this paper proposes a new method for calculating the output characteristics of electromagnetic devices. The following conclusions are obtained:

a) In terms of computational efficiency, in the case of a coil voltage and an rotation angle of armature of the above mentioned clapper-type electromagnetic relay, it takes about 3.2 minutes to calculate the electromagnetic torque by the finite element method. The calculation takes only 0.412 seconds to use the multi-kernel radial basis neural network proposed in this paper. (Note: The computer performance used in this example calculation process is dual-kernel CPU frequency 2.6GHz, memory 8GB). The superiority of the proposed method is reflected in the extremely high computational efficiency of such calculations.

b) In terms of computational accuracy, it is greatly improved by the multi-kernel RBF neural network. This is because the method uses the result of finite element calculation as the sample input, and the global accuracy of electromagnetic torque calculation based on multi-kernel radial basis neural network is obviously better than any single-kernel radial basis neural network. This is mainly due to the advantages of each single-kernel RBF neural network being synthesized by the MK-RBF neural network through different weight coefficients.

c) In terms of the scope of application of the model, the calculation method proposed in this paper can also be used in other fields of nonlinear engineering calculation. The method of multi-kernel RBF neural networks is obviously more applicable than single-kernel RBF neural networks. The method solves the weight value of each single-kernel RBF model by heuristic weighting strategy, which reduces the requirements of the modeler's own level in the modeling process.

REFERENCES

[1] A. Saha and, T. Ray, "Practical robust design optimization using evolutionary algorithms," *Journal of Mechanical Design*, vol. 133, no. 10, pp. 101012.1-101012.19, Oct. 2011.

[2] M. Amrhein and T. Krein, "Induction machine modeling approach based on 3-D magnetic equivalent circuit framework," *IEEE Trans. Magn.*, vol. 25, no. 2, pp. 339-347, May 2010.

[3] L. Encica, J. Makarovic, E. A. Lomonova, and A. J. A. Vandenput, "Space mapping optimization of a cylindrical voice coil actuator," *IEEE Transactions on Industry Application*, vol. 42, no. 6, pp. 1437-1444, Nov. 2006.

[4] B. Xia, Z. Ren, and C.-S. Koh, "Utilizing kriging surrogate models for multi-objective robust optimization of electromagnetic devices," *IEEE Trans. Magn.*, vol. 50, no. 2, pp. 835-838, Feb. 2014.

[5] Y. Xuerong, D. Jie, W. Yingqi, and Z. Guofu, "An approximate calculation model for electromagnetic device based on user-defined interpolating function," *Journal of Magnetics*, vol. 19, no. 4, pp. 378-384, Dec. 2014.

[6] H. A. Tayebi, M. Ghanei, K. Aghajani, and M. Zohrevandi, "Modeling of reactive orange 16 dye removal from aqueous media by mesoporous silica/crosslinked polymer hybrid using RBF, MLP and GMDH neural network models," *Journal of Molecular Structure*, vol. 1178, pp. 514-523, Feb. 2019.

[7] H. K. Ghritlahre and R. K. Prasad, "Exergetic performance prediction of solar air heater using MLP, GRNN and RBF models of artificial neural network technique," *Journal of Environmental*

Management, vol. 223, pp. 566-575, Oct. 2018.

[8] N. Benbouza, F. Z. Louai, and N. Nait-Said, "Application of meshless Petrov Galerkin (MLPG) method in electromagnetic using radial basis functions," *4th IET Conference on Power Electronics, Machines and Drives*, May 2008.

[9] Q. Junfei, M. Xi, and L. Wenjing, "An incremental neuronal-activity-based RBF neural network for nonlinear system modeling," *Neurocomputing*, vol. 302, pp. 1-11, Aug. 2018.

[10] J. W. Perram, "Criterion for the validity of D'Alembert's equations of motion," *Advances in Quantum Chemistry*, vol. 75, pp. 103-116, 2017.

[11] M. Stein, "Large sample properties of simulations using Latin hypercube sampling," *Technometrics*, vol. 29, no. 2, pp. 143-151, 1987.

[12] A. Capozzoli, O. Kilic, C. Curcio, and A. Liseno, "The success of GPU computing in applied electromagnetics," *ACES Journal*, vol. 33, no. 2, pp. 148-151, Feb. 2018.

[13] Z. Guofu, W. Qiya, and R. Wanbin, "An output space-mapping algorithm to optimize the dimensional parameter of electromagnetic relay," *IEEE Trans. Magn.*, vol. 47, no. 9, pp. 2194-2199, Sep. 2011.

[14] R. K. Gordon and W. E. Hutchcraft, "The use of multiquadric radial basis functions in open region problems," *ACES Journal*, vol. 21, no. 2, pp. 127-134, July 2006.

[15] R. K. Gordon and W. E. Hutchcraft, "Comparison of solution accuracy using different sets of radial basis functions," *25th Annual Review of Progress in ACES*, pp. 413-418, Mar. 2009.

Feng Ding received his M.E. degree and the Ph.D. degree in Mechanical Engineering from Xi'an Jiaotong University, China. He is a Professor of the Department of Mechanical and Electronic Engineering, Xi'an Technological University, China. His research interests include condition monitoring, intelligent diagnosis and prognostics, reliability engineering.

Yunyun Gao is a M.E. candidate in the Department of Mechanical and Electronic Engineering, Xi'an Technological University, Xi'an, China. His research interests include structural design, simulation and optimization of mechanical equipment, and numerical algorithm theory.

Jianhui Tian received his Ph.D. degree in Mechanical Design and Theory from Hunan University, China. He is an Associate Professor of the Department of Mechanical and Electronic Engineering, Xi'an Technological University, China. His research interests include engineering optimization design and simulation technology.